Concatenation of Modified Spiral Curve Phase Precoding with New TCM / Turbo Codes for Frequency Selective Fading Channels

Keattisak Sripimanwat
National Electronics and Computer Technology Center (NECTEC),.NSTDA
Science Park, Thailand. Email:ksripima@ieee.org

R.M.A.P. Rajatheva
Department of Electronics & Telecommunications Engineering
University of Moratuwa, Moratuwa, Sri Lanka

Abstract

In this paper, the concatenation of modified phase precoding on a spiral curve technique and new trellis coded modulation (TCM) is proposed for application in the frequency selective slow fading channel of wireless communications. Simulations show a significant improvement of the total gain compared to those of the conventional *post*-equalization of sub-optimum soft output equalizer (SSE) with the same TCM schemes. The modification on the original spiral curve-precoding gives 0.5 dB of gain over the whole range of signal to noise ratio (SNR) including the overcoming of signal amplitude fluctuation in a non-deep fade channel. Next, new TCM codes by the symbol mapping method perform better than the conventional TCM in both of AWGN, and in intersymbol interference (ISI) channels with precoding. The performance of this proposed system is further improved achieving a few dB of gain by the application of soft output detection to each of the codes. A theoretical analysis is carried out to verify the simulation result and found that they match quite well. Finally, the additional result of an adoption of a simple turbo code confirms the success of this ISI combating model as well.

Keywords: Phase Precoding, Trellis Coded Modulation, Turbo Coding, Intersymbol Interference

1. Introduction

Many equalization techniques have been used to combat ISI in wireless communications such as the Viterbi or maximum likelihood equalizer, optimum or sub-optimum-soft output equalizer (OSE,SSE) [1], decision feed back equalizer (DFE), and *pre*-equalizer by using *precoding* techniques. The earliest form of precoding is known as Tomlinson-Harashima (TH) precoding [2][3]. TH-precoding has been used successfully in voice band communications where the channel impulse response is time invariant. Although it is very suitable for pulse and quadrature amplitude modulation (PAM/ - QAM) and there is an attempt to apply it with the continuous wave modulation as in [4], it cannot be applied directly to the time-varying fading channels. Because TH-precoding *pre*-distorts the transmitted signal amplitude, this effect is particularly undesirable for phase modulation, where the constant transmitted signal amplitude is required. Therefore, a modification of precoding for phase modulation is necessary. Consequently, spiral curve-phase precoding [5] has been devised to avoid the disadvantage of TH-precoding by precoding only the carrier phase in order to ensure precoding stability and to achieve an ISI-*free* received signal by keeping the transmitted signal amplitude constant. The results applying this technique show improvements in the slow varying Rician and Rayleigh fading channels. Precoding can be considered as an ideal DFE equalizer at the transmitter. Its importance is recognized since the implementation of DFE

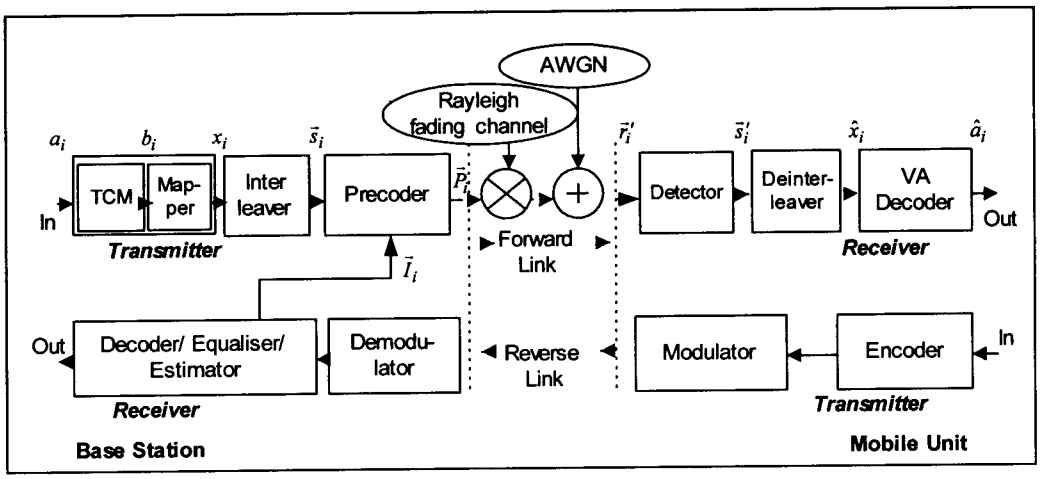

Fig. 1 Proposed Transmission Model

with a Viterbi decoder (VA) at the receiver in order to decode a TCM signal, performs poorly due to the error propagation and inherent decision delays of DFE [6]. In contrast, a Viterbi decoder can be applied in a straightforward way to precoded TCM signals. The combination is expected to improve the overall performance substantially compared to the coded transmission operating on systems with a DFE in the receiver. In this paper, a proposed wireless-transmission model by concatenation of phase precoding and bandwidth-preserving TCM code is introduced. Their performances are compared to another well-known *post*-equalization technique of SSE with the same TCM. In addition, phase precoding and TCM schemes are also developed separately for improving their individual performance. This leads to the formulation of a modified version for phase precoding and an improved TCM constructing method. Moreover, the application of soft output detection for more decoding reliability is presented including the simulation verification by theoretical analysis. This is also with the adoption of turbo code into this proposed model for an additional verification.

2. System and Channel Model

The Spiral curve-phase precoding technique has been already known widely. Moreover, it has been applied to other transmission systems as shown in [7]. Therefore, in this section phase precoding is given only for its concept and the simplification method. The modification technique will be proposed in the next section.

Next, Fig.1 shows the proposed transmission model that consists of a full duplex operation of two signal links. First, TCM encoder generates an $(n + r)$-bit code vector $b_i = (b_i^1,..., b_i^{n+r})$ on the forward link from an n-bit information vector $a_i = (a_i^1,..., a_i^n)$. Each code vector is then mapped onto a complex symbol x_i out of a 2^{n+r}-point **P**hase **S**hift **K**eying constellation and it is interleaved to spread the burst errors. The waveform at the input of the precoder is:

$$s(t) = \sum_i x_i f(t - iT) \qquad (1)$$

where x_i represents the TCM-coded signal constellation and $f(t)$ is a rectangular waveform over $[0, T]$.The signal $s(t)$ can be represented by a sequence of complex-valued samples with the signal envelope $\bar{s}_i$ as in [5].

$$\bar{s}_i = Ae^{j\beta} \qquad (2)$$

where A is the "constant" amplitude, β_i is the carrier phase of a *m-ary* PSK signal. These $\bar{s}_i$ values are precoded into the constant amplitude complex signal values $\bar{P}_i$ in order to compensate the effect of channel ISI $\bar{I}_i$.This precoded signal $\bar{P}_i$ can be evaluated, if the ISI component $\bar{I}_i$ and the desired received signal $\bar{r}_i$ are known by neglecting noise for the present as denoted in equation (3a). The ISI component $\bar{I}_i$ is obtained by an estimation based on the reverse link

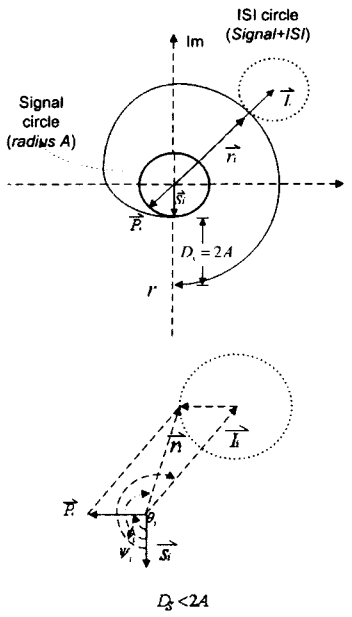

Fig. 2 Simplified Spiral Curve for Phase Precoding

reception and consists of several previous transmitted signal values $\bar{P}_{i-l}$. They are weighted by fading coefficients h_l as shown in (3b):

$$\bar{P}_i = \bar{r}_i - \bar{I}_i \qquad (3a)$$

$$\bar{I}_i = \sum_{l=1}^{L} h_l \bar{P}_{i-l} = i_i e^{j\psi_i} \qquad (3b)$$

i_i and ψ_i are the amplitude and phase of the resulting ISI component at time i, and $\bar{P}_{i-l} = Ae^{j\theta_{i-l}}$ are the previous precoded signal values, where θ_i is the carrier phase after *pre*-distortion ($\bar{P}_i$ can be computed by using the spiral curve method of the next sub-section), and L is the number of tap in ISI T-space model. Hence, the received signal sample after carrier recovery and matched filtering can be described by:

$$\bar{r}_i = \bar{P}_i + \bar{I}_i + \bar{n}_i = Ae^{j\theta_i} + i_i e^{j\psi_i} + \bar{n}_i = r_i e^{j\phi_i} \qquad (4)$$

where $\bar{n}_i$ is an equivalent complex additive white Gaussian noise (AWGN) with zero mean and variance $2\sigma^2$. r_i is the received signal amplitude with phase ϕ_i. It can be explained as a superposition of delayed versions of $\bar{P}_i$ as:

$$\bar{r}_i = \sum_{l=1}^{L} h_l \bar{P}_{i-l} + h_0 \bar{P}_i + \bar{n}_i \qquad (5)$$

where h_0 is the channel impulse response component of the first path. In reality, the system is operated following the assumption that the time division duplex (TDD) scheme is used for both forward and reverse links sharing the same RF channel with different time slots. Next, the channel fades so slowly such that it is assumed to be time invariant over two adjacent frames of the forward and reverse link. Finally, the channel impulse response can be modeled as linear and time-invariant over two adjacent data frames so that the radiation patterns are reciprocal in both forward and reverse links [5][8]. Due to the limitation of size and power consumption of the mobile unit, precoding is used only at the transmitter of the base station.

2.1 Simplified Phase Precoding

To simplify precoding calculations as in [7], the signal amplitude (A) is normalized to be unity and the distance between any two points of 2π -difference is set as $D_s = 2A$. This simplification is shown in Fig. 2. Therefore, the source symbols $\bar{s}_i$ can be estimated exactly at the receiver, if $\bar{r}_i$ is located on this spiral curve, where r_i, ϕ_i, and β_i are related by the following equations:

$$r_i = \frac{A}{a_0} + \frac{A}{a_0}\frac{(\beta_i - \phi_i - \psi_0)}{C\pi} \qquad (6a)$$

$$r_i = C + (\beta_i - \phi_i - \psi_0)/\pi \qquad (6b)$$

where a_0 is the amplitude of first path fading and its phase ψ_0, and C is a spiral curve constant to be equal to the inverse value of a_0. The first term of (6a) is the radius of signal circle and the second is the additional distance to the selected point on a spiral curve. The goal of phase precoding is to preserve constant amplitude of the transmitted signal $\bar{P}_i$. Thus, all $\bar{P}_i$ should be placed on the circle centered at the origin with radius one. In the absence of AWGN, the received signal is on this circle with an ISI offset $\bar{I}_i = i_i e^{j\psi_i}$. A second relation between r_i and ϕ_i can be computed using trigonometric functions resulting in:

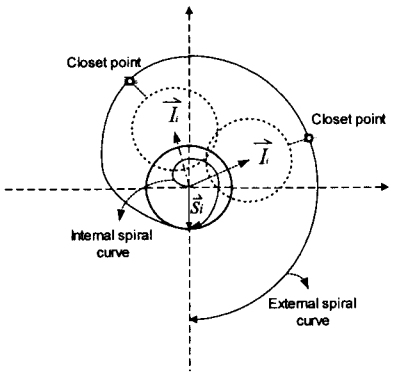

Fig. 3 Modified Spiral Curve for Phase Precoding

$$r_i = i_i \cos(\phi_i - \psi_i) \pm \sqrt{1 - i_i^2 \sin^2(\phi_i - \psi_i)} \qquad (7)$$

Note that all angles in (6) and (7) are absolute values with respect to the spiral curve direction.

The signal $r_i e^{j\phi_i}$ is *pre*-calculated at the transmitter by solving (6) and (7). Then by means of (3a) or (4), the precoded signal $\vec{P}_i = e^{j\phi_i}$ is evaluated (without noise) at the transmitter. At the receiver, the disturbed signal $\vec{r}_i' = r_i' e^{j\phi_i'}$ is detected. Using (6), the information-carrying phase $\hat{\beta}_i$ is calculated by $\hat{\beta}_i = \phi_i' + \psi_0 + (r_i' - C)\pi$ (if there is no noise in the channel, $(\vec{r}_i', \hat{\beta}_i)$ would be the same as the original $(\vec{r}_i, \beta_i)$ showing that ISI is completely erased).The detected signal is then deinterleaved resulting in a sequence of $\hat{x}_i(t)$. Finally, the decoder generates the output sequence $\hat{a}_i(t)$ by means of a VA decoder.

3. Modified Spiral Curve for Phase Precoding

In the previous section, the concatenation of a simplified spiral curve precoding with TCM is proposed. In that transmission system, if no solution could be found for determining the precoded signal from (6) and (7), or if there is no intersection between ISI circle with a spiral curve, a *small amplitude fluctuation* is allowed as in [5] and [7]. In other words, the closet point on the spiral curve from ISI circle will be chosen. That means a constant amplitude signal could not be obtained. To overcome this problem, Automatic Gain Control (AGC) is used in [5]. However, the effect from phase detection error due to the transmitted signal amplitude being forced to be constant by using AGC, causes the detection phase $\hat{\beta}_i$ to be shifted. This angle is related to the received signal amplitude r_i' (or that point on the spiral curve) from (6) and (7), thus, it leads to an equalization error. The above problem is usually found in the deep-fade channel (large effect form a_0) which affects the initialized values of the spiral curve [7]. Even for the non-deep fade channel, the precoding solution may not be obtained by using the *small amplitude fluctuation* concept of [5]. This special case is illustrated in Fig. 3. When the power of ISI is small and ISI circle appears in the first loop of a spiral curve (*"0"* to *"2π"*) as shown by the dashed-line circles. Obviously, there is no cross point of ISI circles with a spiral curve, so that the solution for a precoded signal can not be found. Since a *small amplitude fluctuation* is allowed, the *"closet"* point on spiral curve will be chosen instead. Thus, a precoded signal is obtained but the amplitude of the precoded signal can not be kept constant. To eliminate this drawback without using AGC, an *"internal spiral curve"* is implemented with a new curve in the centered-circle where a new relation of r_i, ϕ_i and β_i for precoding is established by:

$$r_{i,in} = \frac{A}{\rho}\left(1 + \frac{\beta_i - \phi_i}{C_{in}\pi}\right) \qquad (8)$$

where the previous spiral curve is re-named to be the *"external spiral curve"*, ρ is a number proportional to the amplitude A, and C_{in} is the fixed internal spiral curve constant. The ending point of an internal spiral curve is fixed at A, thus, the value of (A/ρ) in (8) suggests the beginning of the non-zero value of an internal spiral curve. To maximize this curve length to obtain a large received amplitude signal of (8) at the receiver, ρ is set at a value of 10. Therefore, the related internal spiral curve constant C_{in} where the intersection point of ISI circles with either internal or external spiral curves can be found, is 2/9. Using this internal spiral curve which considers the first path fading and the normalized amplitude from section 2, gives:

$$r_{i,in} = \frac{C}{\rho}\left(1 + \frac{\beta_i - \phi_i - \psi_0}{C_{in}\pi}\right) \qquad (9)$$

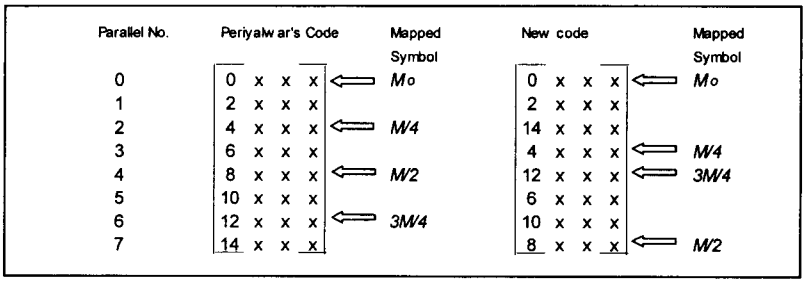

Fig. 4 An Example of *Symbol Mapping* on a Signal Subset of New Code Compared to a Signal Subset of *Periyalwar*'s Code at *Rb* of 1 bit/s/Hz (*k* is 4)

These internal and external precoded signals can be identified at the receiver by comparing the received amplitude in (4) with normalized amplitude A. In a non-deep fade channel with the small effect from a_0, this modified spiral curve can be used to keep the amplitude of transmitted signal constant. This overcomes the drawback of the original version. Moreover, it is found that the received phase of (9) is higher in accuracy than the received phase of (6). It is also for the deep fade channel which contains a large effect from a_0. This improved result is shown in section 6. Consequently, this modified spiral curve precoding is used throughout this paper.

4. New TCM Scheme with Symbol Mapping

Trellis coded modulation (TCM) [9] is very attractive for wireless communications where high spectral efficiency is needed due to the limitation in bandwidth and the power consumption of the mobile unit. The TCM design-parameters which play an important role for relieving fading effect, are the product distance "P_d" and the shortest error event path or time diversity "L" (in additive white Gaussian noise (AWGN) channels, the parameter of importance is the squared Euclidean distance d^2_{free}.). Next, it is found that multiple TCM (MTCM) is more suitable for fading channel where a larger of P_d and L can be achieved. The improved version of MTCM has been presented in [11]. In [12], MTCM scheme has been extensively devised where all above three parameters are already optimized. Therefore, the design rules for optimizing new code become more clear in the sense that focusing only on the signal subset would not give a better code. In this paper, the improvement of TCM is carried out on another part of TCM's set partitioning, that is, on *"mapping"*.

4.1 Symbol Mapping Definition

To map the optimum signal subset (maximized d^2_{free}, "P_d" and "L") on the suitable modulation symbols, use the assumption that *"most errors occur in the adjacent symbols. In order to decrease the detection error on this probable error events, the adjacent code sequence of each signal subset, therefore, should be mapped onto the closer symbol of the previous one without the catastrophic error"*. This method can be described by considering the signal constellation [13]. That is, if symbol zero of M phase modulation was sent, the probability of received symbol M, P_M = $P(received \mid$ symbol M was sent) should satisfy the following relationship:

$$P_0 > P_1 = P_{M-1} > .... > P_{M/2-1} = P_{M/2+1} > P_{M/2} \quad (10)$$

According to the above mapping definition, the new TCM code must follow (10). That means, code sequence b_i in encoder module of Fig.1 should be designed sequentially from the zero parallel and/or zero state transition up to the maximum parallel and/or the maximum state transition. For mapping each code on the symbol x_i, it starts at the zero-symbol, the adjacent symbol of *1*, and *M-1*, and ends up at the *M/2* symbol. For the above definition, computer programming is an efficient method to search for a good code. It has been done as an algorithm for TCM set partitioning which satisfies with (10). As a result, several new codes are devised (They are listed in the appendix). An example of these new codes is illustrated in Fig 4 with a 4MTCM-16PSK signal subset at a throughput (*Rb*) of 1 bit/s/Hz and multiple (*k*) of four.

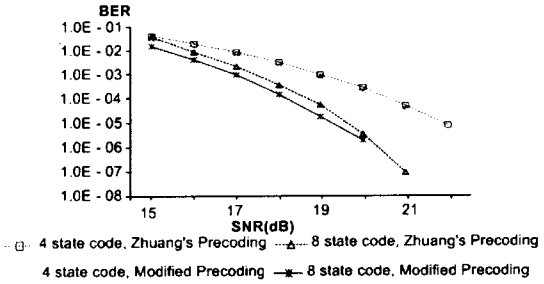

Fig. 5 Performance of Modified Spiral Curve with TCM-8PSK, Rate 2/3

Signal subset of new code is compared to a subset of *Periyalwar*'s code [11] with the same parameters of d^2_{free}, P_d and L_{min}. To simplify this comparison, That only the first columns (k=1) in each signal subset of both codes (these subsets contain eight parallel transitions) are considered. They show that this new code holds higher possibility of signal subsets that are mapped onto the suitable symbols following TCM set partitioning without catastrophic error because these mapped symbols follow Equation (10) whereas *Periyalwar*'s mapped symbols do not. Note that for *M*TCM encoding, *symbol mapping* process in Fig. 4 is done on every multiple (k) of each signal subset.

It is specially noted that this symbol mapping is done on the set partitioning process (*joint* encoding and modulation with mapping) of the TCM encoder. This is different to those of the general *Gray* mapping method which is applied for the uncoded signal or even for the coded signal where the encoding and mapping processes are considered *separately*.

5. Soft Precoded-Signal Detection

It was known that for a communication system consisting of two sequence estimation modules in a serial receiver, the outer module should provide the inner module with soft information in order to improve the system performance [14]. Therefore, if the precoded signal detector in Fig.1 could give soft output information for the soft input VA decoder, a further performance improvement is expected.

Referring to the perfect ISI combating or ISI-*free* signal as in [5], let $s_{p\_sim.} = (C\pi n_{ri})/A$ be a simplified *spiral*-Gaussian random variable of [15] of the detection phase error $\Delta\beta = \hat{\beta}_i - \beta_i$ from reorganization of (6) where n_{ri} is an independent *amplitude*-Gaussian random variable of the i^{th} received signal of a Rayleigh distribution with zero mean and variance σ^2. This variable is simplified in such a way that the independent *phase*-Gaussian random variable $n_{\phi i}$ from [15] can be neglected due to its small effect at high signal to noise ratio (SNR). The mean of this s_{p_sim} is zero and variance $\sigma^2{}_{sp\_sim}$ is $(C\pi/A)^2\sigma^2$. The *pdf* of s_{p_sim} is thus:

$$p(s_{p\_sim}) = \frac{1}{\sigma_{sp\_sim}\sqrt{2\pi}} \exp[(-1/2)(s_{p\_sim}/\sigma_{sp\_sim})^2] \quad (11a)$$

Therefore, soft output information of i^{th} received signal is taken from the conditional *pdf* of:

$$p_{sim}(r_i'|s_i^m) = \left(\frac{1}{\sigma_{sp\_sim}\sqrt{2\pi}}\right) \exp\left[-\frac{|r_i' - s_i^m|^2}{2\sigma^2{}_{sp\_sim}}\right] \quad (11b)$$

where m is 0, 1, 2, .., M-1.

6. Simulation Results and Evaluations

The simulated ISI channel of this paper is modeled by two equal strength rays of Rayleigh fading on the τ-spaced discrete-time model where the delay $\tau = |\tau_1(t) - \tau_0(t)|$ is one symbol period T. The tap gain h_l of the channel impulse response in (5) is generated by a zero-mean complex Gaussian random process of the filtered Gaussian noise method [16]. In this work, Doppler effect is *not* taken into account. In this section, the performance of the modified spiral curve precoding concatenated with TCM code in the transmitter using a normal (or hard) detection scheme named as *system I*, is evaluated compared to a system that uses a simple SSE in the receiver with the same TCM code (*system II*). This SSE is a soft output *post*-equalization method that has been applied successfully for combating ISI in [2][17]. It has several advantages, as noise variance is not required, simulation programming is less complex because computations are processed in a logarithmic domain, and the well-known add-compare - select (ACS) algorithm is the main

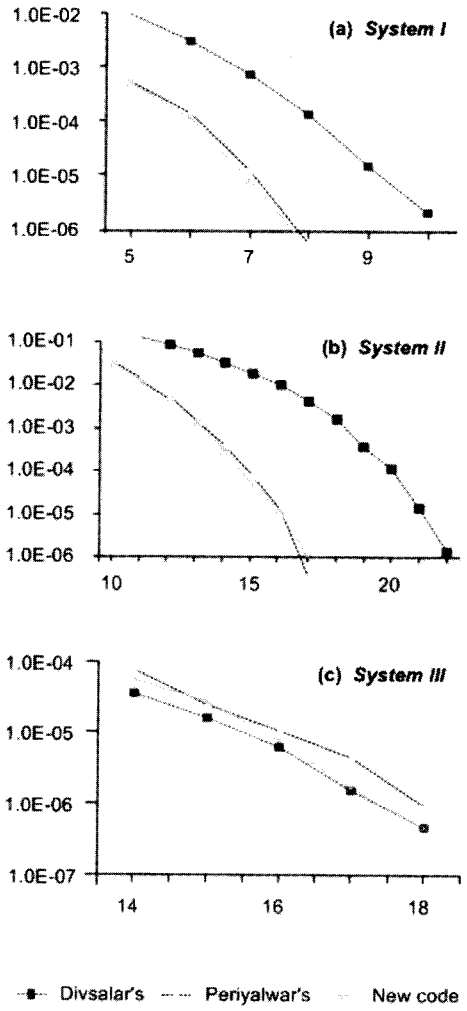

Fig. 6 BER as a Function of SNR (dB) with *Rb*=1 TCM Codes

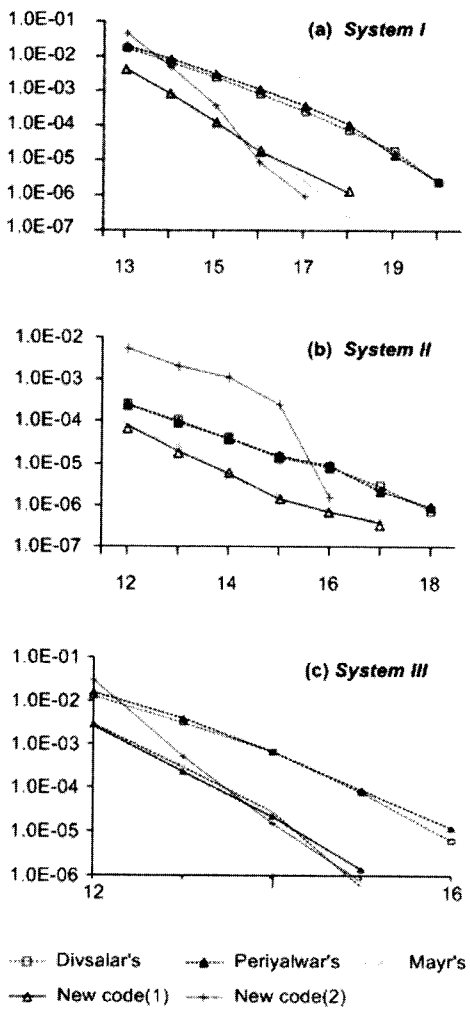

Fig. 7 BER as a Function of SNR (dB) with *Rb*=1.5 TCM Codes

operation as in the conventional Viterbi algorithm (VA). In this paper, decision delay D at the value of 6 is chosen for this SSE-system. Next, the result of *system I* with soft precoded-signal detection scheme named as "*system III*" will be compared with all of the previous system performances. First, for an AWGN channel the performance of a new TCM scheme is investigated compared to the conventional code's. It is found that all new TCM codes perform in this channel better than the given codes in the literature as summarized in Table 1. (It is noted that performance comparison is done at 10^{-5} and 10^{-6} of bit error rate (BER) for AWGN and ISI channel respectively). Next for an ISI channel, it is started with the original spiral curve precoding concatenated with 4 states and 8 states of *Ungerboeck*'s TCM codes [9] (*Rb* of 2). They are tested and compared to the modified precoding with the same TCM. Their results in Fig.5 show that the modified spiral curve has a gain of 0.5 dB compared to the original version over the whole SNR range. Therefore, this modified precoding is more effective. Subsequently, the combination of this modified precoding with various codes of new TCM scheme is considered. The result of new code (d^2_{free}=8, P_d=4, L=4) with *Rb* of 1 is simulated and compared to *Periyalwar*'s code [11] with the same design-parameters and with *Divsalar*'s code [10] which has a smaller d^2_{free}

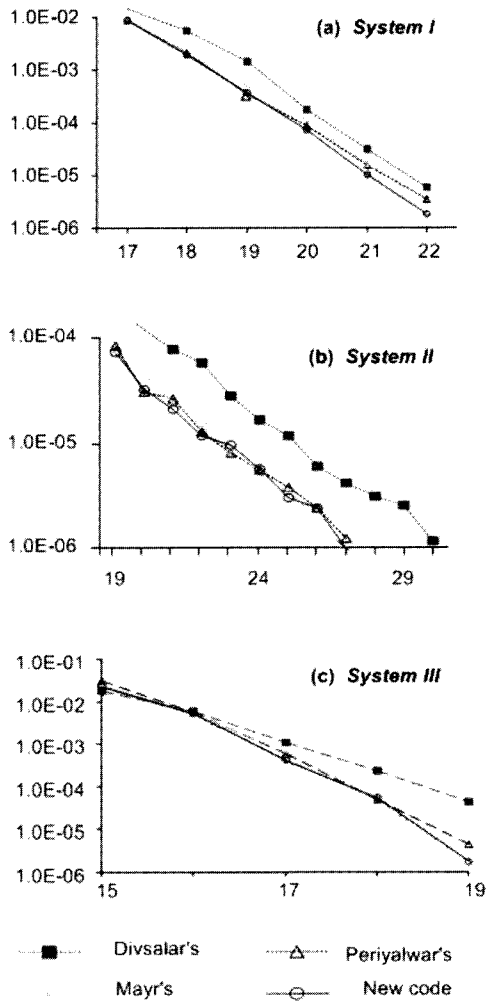

Fig. 8 BER as a Function of SNR (dB) with *Rb*=2.5 TCM Codes

(4.69). In Fig. 6, new code shows that it has an equal effective as *Periyalwar*'s code on *system I* and it has 2 dB of gain compared to *Divsalar*'s. For *system II*, new code performance is equal to *Divsalar*'s and 1 dB gain is achieved compared to *Periyalwar*'s. The performance of new code in *system I* tends to have a larger gain compared to *system II*'s at a low BER. Furthermore, soft output detection in *system III* gives an additional gain of about 0.8 dB from those of *system I*. Two new codes with *Rb* of 1.5 have been constructed. They perform quite different as shown in Fig.7. New code version (1) (d^2_{free}=8, P_d=4, L=4) performs well at low SNR, but at high SNR new code version (2) (d^2_{free}=8, P_d=4, L=4) is the best on both *system I* and *system II*. This is compared to *Mayr*'s code (d^2_{free}=8, P_d=4, L=4) [12], *Periyalwar*'s (d^2_{free}=8, P_d=8, and L=3), as well as *Divsalar*'s (d^2_{free}=5.17, P_d=8, L=3). At this *Rb*, *system I* performs poorer than *system II* but it trends to be better at higher SNR with quite low of BER. By using soft output detection in *system III*, almost 3 dB of gain is further achieved compared to previous result of *system I* and it is also better than *system II*. New code, *Mayr*'s code, and *Periyalwar*'s code perform, however, rather similar in the *system III*. At *Rb* of 2.5, the *system I* gains about 4 dB from those of *system II*. The result is shown in Fig. 8. An attractive further gain of 3 dB is achieved with *system III*. New code (d^2_{free}=2.34, P_d=2, L=2) performs equally with *Mayr*'s code and has slightly better performance than other codes with the same design parameters. Finally at in *Rb* of 3, performance of the new code (d^2_{free}=0.89, P_d=1.17, L=2) as shown in Fig.9, is compared to the result of *Mayr*'s code with the same design parameters. It achieves a better gain in *system I* and in *system III*. However, in *system II* the performance of new code equals to that of *Mayr*'s code. The combined gain of new code in *system I* compared to those of the *system II* is 2 dB. Moreover, up to 3.5 dB of gain is further achieved from *system III* by using soft output detection. In summary, all new codes have shown a better performance than those given in the literature when they are applied for AWGN channel. This is because of the advantage of *symbol mapping*. For an application in ISI channel, this advantage is diminished when it is used with the SSE equalizer as in the *system II*. It is due to the fact that there is no time diversity "*L*" improvement by the *symbol mapping* method. The advantage of the new codes is realized only in AWGN and in its *equivalent* channel. Both of *system I* and system *III* are considered as an ISI-*free* or the "*equivalent*-AWGN" channel, where the effect of only AWGN remains. Therefore, this explains the effectiveness of *symbol mapping* on ISI channel for the precoded system. In addition, the application of soft precoded signal detection is another successful technique. It leads to a better decoding result or a higher gain at the output. Note that, although the pure gain of new TCM codes compared to the given codes is not much (maximum 1 dB at *Rb* of 3 with system *III*), this improved gain along with the performance of

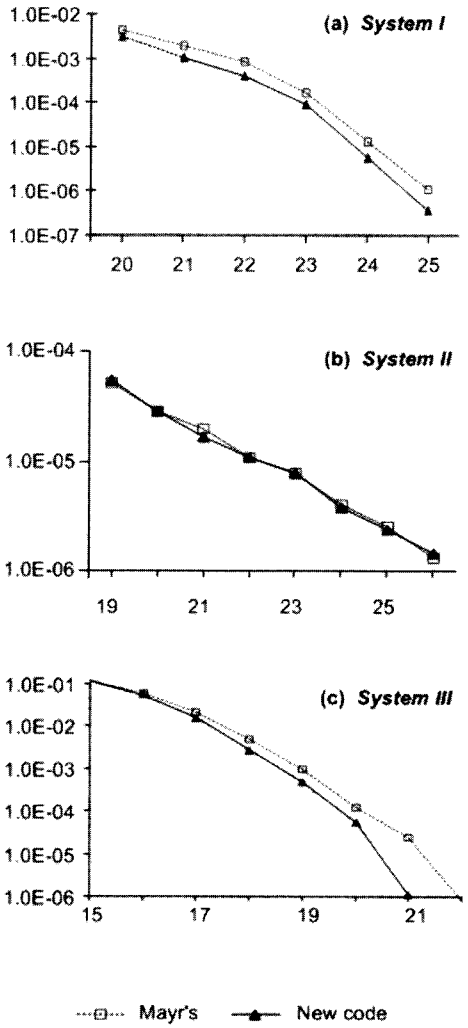

Fig. 9 BER as a Function of SNR (dB) with *Rb*=3 TCM Codes

modified phase precoding scheme obtains a very significant gain. That is up to 7 dB and 5.5 dB at *Rb* of 2.5 and 3 respectively. Finally, all new codes design parameters and their performances in both AWGN and ISI channel are given in Table 1.

7. Performance Analysis

Previously, there has been an improved analysis for pure spiral curve precoding proposed in [18]. In that work, the original analysis of [5] is upgraded including the extension from only QPSK to higher modulation signals (8, 16, and 32PSK). To continue for using with the proposed concatenation system of this paper, it is also assumed that there is an intersection point of a spiral curve with the ISI-circle on each transmitted signal. This is done by using a large value for spiral curve constant C for obtaining a small 2π-difference distance on a spiral curve ($D_s \le 2A$) (C is large enough such that the internal spiral curve can be neglected). It is noted that a higher possibility of getting a cross point is achieved by using a large value of C. Nevertheless, the sensitivity to noise is also higher. Next, to consider a code sequence $B = b_1, b_2, .., b_i$ which is mapped on to a symbol sequence $X = x_1, x_2, .., x_i$ by $F(b_i) = x_i$ at TCM encoder module of Fig. 1. The symbol error probability P_e due to the code sequence B plus error sequence E_L of length L on a trellis can be described by a node error event [19][20] as follows:

$$P_e = \sum_{L=1}^{\infty} \sum_{B} P\{B\} \sum_{E_L \neq 0} P\{B \rightarrow B \oplus E_L\} \qquad (12)$$

It is assumed that the ISI effect is completely eliminated by phase precoding. Then, the channel is perturbed only by *spiral*–Gaussian noise with a two-sided noise spectral density $N_{o,spiral\_sim}/2E_s$, and $E_s = nE_b$ (This is computed from a simplified *spiral*-Gaussian random variable in section 5). Similar to the derivation in pure AWGN channel [19], the symbol error probability is then upper bounded as:

$$P_e \le Q\left(\sqrt{\frac{d^2_{free} E_s}{2N_{o,spiral\_sim}}}\right) \exp\left(\frac{d^2_{free} E_s}{4N_{0,spiral\_sim}}\right) \sum_{L=1}^{\alpha} \sum_{B} P\{B\} \cdot \sum_{E_L \neq 0} \exp\left\{-\frac{E_s \left\| F(B) - F(B \oplus E_L) \right\|}{4N_{0,spiral\_sim}}\right\} \qquad (13)$$

where $Q(z) = \int_{z}^{\infty} (1/\sqrt{2\pi}) \exp(-t^2/2) dt$. The last multiple term of (13) is generally known as the transfer function *T(D)* of TCM code. Finally, bit error probability can be obtained after getting *T(D)* as:

$$P_b \le \frac{1}{n} Q\left(\sqrt{\frac{d^2_{free} E_s}{2N_{o,spiral\_sim}}}\right) \exp\left(\frac{d^2_{free} E_s}{4N_{0,spiral\_sim}}\right) \cdot \left. \frac{\partial T(D,I)}{\partial I} \right|_{D=\exp(-E_s/4N_{0,spiral\_sim}), I=1} \qquad (14)$$

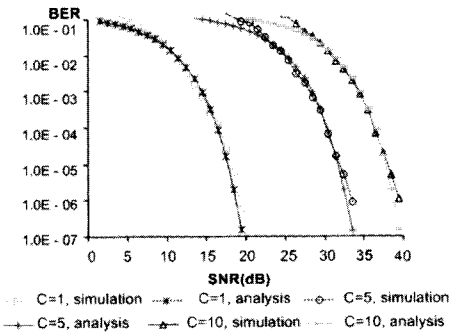

Fig. 10 Performance Comparison of QPSK-TCM (Rb=1) with Precoding

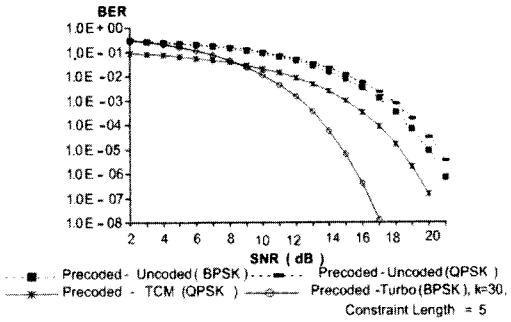

Fig. 11 Performance Comparison of Turbo Codes with Precoding (C=1)

Similarly, bit error probability of MTCM can be obtained by replacing "n" by "b" and $E_s / N_{o,spiral\_sim} = (b/k)E_b / N_{o,spiral\_sim}$, where b is the number of MTCM encoder input bit and k is the multiplicity. An example for this proposed analysis is given by a conventional two states QPSK-TCM code (Rb=1) [19,p 103]. This analysis result is compared to its simulation result in Fig.10 with different values of the spiral curve constant C. It shows that the result from (14) verify the simulation performance of the precoded-TCM signal with soft output detection very well.

8. Further Application of Turbo Codes

To consider for the further contribution of this work, new TCM constructing method of this paper can be applied to many applications such as for an unequal error protection scheme (UEP) in which the different throughput-sources or variable rate transmission is required, and for the adaptive TCM scheme in the automatic repeat request (ARQ) system. Furthermore, the development of other high-quality coding method of turbo code [21] concatenating with this modified spiral-curve phase precoding is also promising. In this section, the application of simple turbo codes with the proposed system is investigated. Referring to the same transmitted model of Fig. 1, TCM is now removed with the using of turbo codes instead. However, all of the previous assumptions are still adopted. In this investigation, it is done by the analysis method and its result will be compared to the previous performance of the TCM with the same precoding scheme.

In order to achieve the numerical result for this analysis, the upper bound of linear small block turbo codes is considered and adopted from [22]. This method is to count for the weight distribution related to the codes word's Hamming weight, which is feasible for the small information block size. For simplifying this investigation, only BPSK signaling is considered including the use of maximum likelihood decoding based on the uniform interleaving assumption. Thus, the general upper bound of turbo codes with spiral phase precoding is computed from the probability of codeword error (PCE) of [22]:

$$P_e \approx\leq \sum_{w=d_{\min}} C_w Q\left(\sqrt{\frac{2E_b}{N_{o,Spiral}} R_c w}\right) \qquad (15)$$

where R_c is the coding rate, w_m is the Hamming weight of code word m, C_w is an integer of weight distribution corresponding to the number of code words $w \in [1,n]$. Normally, the performance measurement is considered on the weight distribution of the first *non*-zero element (the *minimum distance* code word; d_{min}). However at high signal to noise ratio (SNR), *the most* significant contribution to overall code word error probability is that the *lowest*-weight code word. To achieve the result from this upper bound, the *lowest* counted-weight distribution to the code word's Hamming weight ($C_{w=7,\ lowest}$) with its information block size (k) at 30, generating polynomials (23,35), R_c = 1/2, and constraint length (**K**) of 5, is 2 [22]. Next, the result in Fig. 11 (with the same precoding scheme) shows that turbo codes achieve the best system gain compared to those of TCM or the performance of pure uncoded-BPSK and uncoded-QPSK. Although, this simple turbo code has been done at a bit lower throughput

Table. 1 Summary of TCM Codes with their Parameters and Performances

Rb	State	Parallel	k	Tx.Rate	Mod.	Squa.E.D.	Pd	L	SNR(AWGN)	SNR(system I)	SNR(system II)	SNR(system III)	Design.of
1	2	8	4	4|16	4*16	8	4	4	6.9	17	17	16.2	*New*
	2	8	4	4|16	4*16	8	4	4	7	17	18	16.2	Per.
	2	8	4	4|12	4*8	4.69	4	4	9	22	17	20	Div.
1.5	8	1	2	3|6	88	8	4	4	5.8	17.5	16	15	*New(1)*
	8	1	2	3|6	88	8	4	4	5.5	17	16	14.8	*New(2)*
	8	1	2	3|6	88	8	4	4	5.8	18	16	14.8	Mayr.
	8	1	2	3|6	88	8	8	3	7	20.5	18	17	Per.
	8	1	2	3|6	88	5.17	8	3	7	20.5	18	16.5	Div.
2.5	4	8	2	5|8	2*16	2.34	2	2	8.8	22.2	26.6	19.2	*New*
	4	8	2	5|8	2*16	2.34	2	2	9	22.2	26.6	19.2	Mayr.
	4	8	2	5|8	2*16	2.34	2	2	8.9	22.5	27	20	Per.
	4	8	2	5|6	88	1.75	1.17	2	10	23	30	21	Div.
3	8	8	2	6|8	2*16	0.89	1.17	2	11.3	24.5	26.5	21	*New*
	8	8	2	6|8	2*16	0.89	1.17	2	11.5	25	26.5	22	Mayr.

Mayr., Per., and Div. are Mayr's, Periyalwar's, and Divsalar's code respectively.

than those of TCM, it presents the promise of obtaining much higher gain when the optimal turbo codes with the iterative decoding are designed optimally and used. In conclusion, this application of turbo codes also confirms the success of the proposed concatenation system of this paper as well.

9. Conclusions

This paper presents a modified spiral curve precoding technique and a new TCM constructing method with *symbol mapping* definition. In addition, their concatenation model for application in wireless communications through ISI channels is proposed. The individual result from the modification of a spiral curve precoding shows up to 0.5 dB of gain compared to those of the conventional version, including the overcoming of signal amplitude fluctuation in the non-deep fade channel. Next, new TCM codes show an improved performance in both AWGN and some in ISI channel with precoding system. Consequently, the concatenation of this modified spiral curve-phase precoding with new TCM code gives a better gain compared to those of the *post*-equalization of SSE system with the same TCM. Moreover, a few further dB of gain is achieved when the soft output detection method is adopted. Finally, this concatenation system has been verified by theoretical analysis. Its bounds match the simulation result very well. It can be concluded that this proposed transmission system is a successful ISI combating model for wireless communications where phase modulation is preferred. Moreover, the result from an additional investigation of using turbo codes in this system supports this success as well.

10. References

[1] Y. Li, B. Vucetic and Y. Sato, Optimum Soft-Output Detection for Channels with Intersymbol Interference, IEEE Trans. Inform. Theory, Vol. 41, No.3, May 1995, pp.704-713.

[2] M. Tomlinson, New Automatic Equaliser Employing Modulo Arithmetic, *IEE Electronics Letters*, Vol. 7, Mar 1971, pp. 138-139.

[3] H. Harashima and H. Miyakawa, Match-Transmission Technique for Channels with Intersymbol Interference, *IEEE Trans. on Commun.*, Vol. Com-20, August 1972, pp.774-780.

[4] J.P. Meehan and A.D. Fagan, Precoding over Dynamic Continuous wave Digital Mobile Channel, *IEEE PIMRC'97*, Helsinki-Finland, pp. 1140-1144, Sept. 1997.

[5] W. Zhuang and V. Huang, Phase Precoding for Frequency-selective Rayleigh and Rician Slowly Fading Channels, *IEEE Trans. Veh. Technol.*, Vol. 46, No. 1, Feb.1997, pp. 129-142.

[6] J. G. Proakis, *Digital Communications*, (3rd edition) McGraw-Hill, 1995.

[7] K. Sripimanwat, H. Weinrichter, et al, Performance of Concatenated Phase Precoding and TCM on Frequency Selective Fading Channel, *IEEE*

CCECE'2000, Halifax, Canada, May 7-10, 2000.

[8] K.J.Fujimoto, *Mobile Antenna Systems Handbook*, Artech House Inc., 1994, Chap.2.

[9] G. Ungerbeock, Channel Coding with Multilevel Phase Signals, *IEEE Trans. Inform. Theory*, Vol. IT-28, January 1982, pp. 55-67.

[10] D. Divsalar and M.K. Simon, Multiple Trellis Coded Modulation. *IEEE Trans. on Commun.*, Vol. 36, pp. 410-419, No. 4, April 1988.

[11] S. Periyalwar and S.M. Fleisher, A Modified Design of Trellis-Coded MPSK for the Fading Channel, *IEEE Trans. on Commun.*, Vol. 41, No.6, June 1993, pp. 874-882.

[12] B.J. Mayr, *Codiertechniken für den Schwundkanal*, Ph.D Dissertation (in German), Department of Communication and Radio Frequency Engineering, Vienna University of Technology, Austria, 1995.

[13] K Sripimanwat, *Modified Trellis Coded Modulation and Precoding for ISI channel in Wireless Communications,* D.Eng dissertation, Telecommunications program, SAT, AIT, Thailand, 2000.

[14] J. Hagenauer and P. Hoeher, A Viterbi with Soft-Decision Outputs and its Applications, *IEEE Globecom'89 Conf. Rec.*, Vol. 3, pp.1680-1686, 1989.

[15] K. Sripimanwat, et al. Soft-detection Phase precoding with MPSK-TCM for ISI Channel, *IEEE Commun. Letters*, April 2001, pp. 163-165.

[16] G.L. Stuber, *Principles of Mobile Communication*, Boston, Kluwer, 1996, Chapter 2.

[17] Y. Chen, K.B. Letaief and J.C. Chuang, Soft-Output Equalization and TCM for Wireless Personal Communications Systems, *IEEE Journal on Selected Areas in Communications*, Vol. 16, No. 9, pp. 704-713, Dec 1998

[18] K. Sripimanwat, H. Weinrichter, et al, Improved Performance analysis of Spiral Curve-Phase Precoding, *IEE Electronics Letters,* Vol. 36, No.8, pp. 729-730, April 2000.

[19] E . Biglieri, D. Divsalar, P.J. McLane and M.K. Simon, *Introduction to Trellis Coded Modulation with Applications*, Macmillan Pub. 1991.

[20].S.B. Wicker, *Error Control Systems for Digital Communication and Storage*, Prentice Hall Inter, Editions, NJ., 1995.

[21] C. Berrou, A. Glavieux, and P. Thitimajshima, Near Shannon Limit Error-Correcting Coding and Decoding: Turbo-Codes, *Proc. IEEE Int. Conf. Commun., ICC'93*, pp. 1046-1070, May 1993.

[22] K. Sripimanwat, An Upper Bound of Binary Phase Precoding with Turbo Codes in Frequency Selective Fading Channels, PIMRC2001, San Diego, CA, USA, Sept. 30- Oct. 3, 2001.

Appendix:

List of signal subset of new TCM codes:

Rb = 1

New code (1)

Row, (R)= (0 0,1 5,2 2,3 7,7 3,6 6,5 1,4 4)

Column, (C) = (0 0,1 3,2 6,3 1,4 4,5 7,6 2,7 5)

New code (2)

Row, (R) = (0 0,1 3,7 5,2 6,6 2,3 1,5 7,4 4)

Column, (C) = (0 0,1 5,2 2,3 7,7 3,6 6,5 1,4 4)

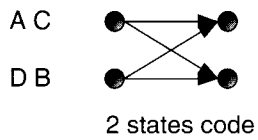

Fig. A1 Trellis Diagram of New TCM *Rb* of 1

Rb=1.5

New code (1)

Row, (R)= (0 0,1 5,2 2,3 7,7 3,6 6,5 1,4 4)

Column, (C) = (0 0,1 3,2 6,3 1,4 4,5 7,6 2,7 5)

New code (2)

Row, (R) = (0 0,1 3,7 5,2 6,6 2,3 1,5 7,4 4)

Column, (C) = (0 0,1 5,2 2,3 7,7 3,6 6,5 1,4 4)

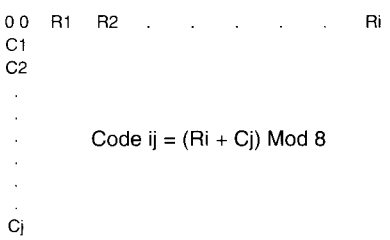

Fig. A2 State Transition Metric (STM)[12] for Generating Signal Subset at *Rb* of 1.5

Rb =2.5

A = (0 0,2 10,4 4,6 14,14 6,12 12,10 2,8 8);
B = (0 12,2 6,4 0,6 10,14 2,12 8,10 14,8 4)
C = (0 4,2 14,4 8,6 2,14 10,12 0,10 6,8 12);
D = (0 8,2 2,4 12,6 6,14 14,12 4,10 10,8 0)
E = (1 5,3 15,5 9,7 3,15 11,13 1,11 7,9 13);
F = (1 1,3 11,5 5,7 15,15 7,13 13,11 3,9 1)
G = (1 9,3 3,5 13,7 7,15 15,13 5,11 11,9 1);
H = (1 13,3 7,5 1,7 11,15 3,13 9,11 15,9 5)

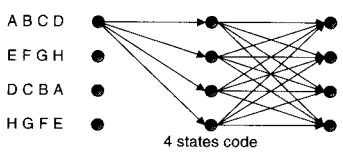

Fig. A3 Trellis Diagram of New TCM *Rb* of 2.5.

Rb = 3

A = (0 0,2 6,4 12,6 2,14 10,12 4,10 14,8 8);
B = (0 2,2 8,4 14,6 4,14 12,12 6,10 0,8 10)
C = (0 4,2 10,4 0,6 6,14 14,12 8,10 2,8 12);
D = (0 6,2 12,4 2,6 8,14 0,12 10,10 4,8 14)
E = (0 8,2 14,4 4,6 10,14 2,12 12,10 6,8 0);
F = (0 10,2 0,4 6,6 12,14 4,12 14,10 8,8 2)
G = (0 12,2 2,4 8,6 14,14 6,12 0,10 10,8 4);
H = (0 14,2 4,4 10,6 0,14 8,12 2,10 12,8 6)
I = (1 1,3 7,5 13,7 3,15 11,13 5,11 15,9 9);
J = (1 3,3 9,5 15,7 5,15 13,13 7,11 1,9 11);
K = (1 5,3 11,5 1,7 7,15 15,13 9,11 3,9 13);
L = (1 7,3 13,5 3,7 9,15 1,13 11,11 5,9 15);
M =(1 9,3 15,5 5,7 11,15 3,13 13,11,7,9,1);

$$\begin{bmatrix} A & B & H & C & G & D & F & E \\ I & J & P & K & O & L & N & M \\ B & A & C & H & D & G & E & F \\ J & I & K & P & L & O & M & N \\ F & E & G & D & H & C & A & B \\ N & M & O & L & P & K & I & J \\ E & F & D & G & C & H & B & A \\ M & N & L & O & K & P & J & I \end{bmatrix}$$

Fig. A4 Signal Subset Metric of New TCM *Rb* of 3